8: ^{1}H NMR δ 6.5–6.7 (m, 6 H), 7.24 (d, 1 H), 7.77–7.94 (m, 4 H), 8.15 (2d, 1 H), 8.35 (br, 1 H); ^{13}C NMR 19 signals total δ 146.4 (C4'), 168.2 (COO^-), 164.6 (amide), 124.2–132.1 (4 benzyl carbons); MS ($C_{27}H_{16}O_8N_2$) calcd 496.07, $M^+ - CO_2$ 452.0 (39.4%); mp 220 °C dec.

9: ^{1}H NMR δ 6.5–6.7 (m, 6 H), 7.26 (d, 1 H), 7.87 (t, 1 H), 8.12 (2d, 1 H), 8.44 (m, 3 H), 8.82 (br, 1 H); ^{13}C NMR 19 signals total δ 146.1 (C4'), 168.3 (COO^-), 163.8 (amide), 124.2–132.1 (4 benzyl carbons); MS ($C_{27}H_{16}O_8N_2$) calcd 496.07, $M^+ - CO_2$ 452.0 (30.5%); mp 247 °C dec.

10: ^{1}H NMR δ 6.5–6.7 (m, 6 H), 7.27 (d, 1 H), 8.11 (2t, 1 H), 8.23 (d, 2 H), 8.37 (d, 2 H), 8.47 (d, 1 H); ^{13}C NMR 19 signals total δ 146.8 (C4'), 168.5 (COO^-), 164.5 (amide), 124.5–127.5 (4 benzyl carbons); MS ($C_{27}H_{16}O_8N_2$) calcd 496.07, $M^+ - CO_2$ 452.0 (55.1%); mp 316 °C dec.

pH Titrations of Fluorescein and Fluoresceinamine. Dye solutions (10^{-5} M) were prepared with 5 mM HCl and titrated with 500 mM NaOH. pH and fluorescence intensity were monitored simultaneously with the Fisher Acumet pH meter and variable-excitation fluorescence spectrometer.

Titration of Fluoresceinamine with Surfactants. Solutions of 0.5 mM fluoresceinamine and 0.5 mM CTAB or Tween 20 were prepared with 100 mM phosphate buffer, pH 7.5. Aliquots of surfactant were added to fluoresceinamine solution, and the generation of fluorescence was monitored with a bare optical fiber in solution, with the instrumentation previously described.

Acknowledgment. We thank William Koshute (Tufts University) and Charles R. Iden (State University of New York, Stony Brook) for the mass spectral determination. This work was supported by a grant from EPA to Tufts Center for Environmental Management.

Determination of Exciton Hopping Rates in Ruthenium(II) Tris(bipyridine) Complexes by Picosecond Polarized Absorption Spectroscopy

Laura F. Cooley,† Pamela Bergquist, and David F. Kelley*

Contribution from the Department of Chemistry, Colorado State University, Fort Collins, Colorado 80523. *Received October 16, 1989*

Abstract: Exciton hopping in excited state $Ru^{II}(bpy)_3$ has been studied in room-temperature solutions with picosecond polarized absorption spectroscopy. Initial excitation is to the metal-to-ligand charge-transfer state (460 nm), and the excited state is probed by polarized 355-nm light. In ethylene glycol the depolarization ratio exhibits a biexponential decay, consisting of 75 ps and 2.4 ns components. The two components of the decay are assigned, respectively, to exciton hopping and to rotational diffusion. The presence of a fast component shows that the optical electron is intrinsically localized on a specific ligand. The amplitudes of the fast and slow polarization decay components may be quantitatively understood in terms of photoselection theory. Exciton hopping in water and methanol solutions occurs much more rapidly than in ethylene glycol. These results are interpreted in terms of solvent-mediated electron-transfer theory.

The photophysics of tris(bipyridine)ruthenium(II), $Ru^{II}(bpy)_3$, have been extensively studied over the past decade. It has long been known that the lowest energy excited state of this complex is metal-to-ligand charge-transfer (MLCT) in nature. It was later established that in room-temperature solutions, the optical electron (i.e., the electron transferred from the metal) is localized on a single bipyridine ligand.[1-4] Since the issue of localization vs delocalization was settled, other questions, regarding the localization time scale and the role of the solvent in the localization process, have been widely debated in the literature. Recent interest has also focussed on the question of the time scale for transfer of the optical electron from one bipyridine ligand to another. This intramolecular electron-transfer process has generally been referred to as "exciton hopping". Since the electronic excitation remains on the same $Ru^{II}(bpy)_3$ molecule, this is a bit of a misnomer. However, in keeping with the precedents in the literature, we will refer to this excited state interligand electron transfer as "exciton hopping".

The results of several experimental studies have been interpreted in terms of initial delocalization of the optical electron. If the exciton is initially delocalized, localization may then occur in concert with solvent relaxation, which stabilizes the nascent dipole (the "solvent-induced localization" model). Magnetic circularly polarized luminescence, time-resolved luminescence, and nanosecond transient Raman results have been interpreted in terms of this model.[5-7] More recently, picosecond transient Raman results on $Ru^{II}(bpy)_3$ in water and in glycerol have also been interpreted to support this model.[8]

Other studies have yielded evidence in contradiction with the solvent-induced localization model. These studies have concluded that the optical electron is intrinsically localized on a single ligand upon absorption of the photon, so that solvent motions are not required to facilitate localization. Solvent dependent shifts in the absorption spectrum of $Ru^{II}(bpy)_3$ have been interpreted in terms of production of a dipole upon absorption of the photon, i.e., intrinsic localization.[9] This mechanism is also strongly supported by photoselection/polarized emission studies in frozen glasses.[4,10-12] Polarizations are obtained which are too large to be explained by a delocalized model. Further support for intrinsic localization also comes from picosecond transient Raman studies.[13] In these

* Author to whom correspondence should be addressed.
† Present address: Physical Sciences Department, Rhode Island College, Providence, RI 02908.

(1) (a) Dallinger, R. F.; Woodruff, W. H. *J. Am. Chem. Soc.* **1979**, *191*, 4391. (b) Bradley, P. G.; Kress, N.; Hornberger, B. A.; Dallinger, R. F.; Woodruff, W. H. *J. Am. Chem. Soc.* **1981**, *103*, 7441.
(2) Forster, M.; Hester, R. E. *Chem. Phys. Lett.* **1981**, *81*, 42.
(3) Holper, W.; DeArmond, M. K. *J.* lumin. **1972**, *5*, 225.
(4) Carlin, C. M.; DeArmond, M. K. *Chem. Phys. Lett.* **1982**, *89*, 297.
(5) (a) Krausz, E. *Chem. Phys. Lett.* **1985**, *116*, 501. (b) Ferguson, J.; Krausz, E. R.; Maeder, M. *J. Phys. Chem.* **1985**, *89*, 1852.
(6) Ferguson, J.; Krausz, E. *Chem. Phys. Lett.* **1986**, *127*, 551.
(7) Tamura, N. K.; Kim, H. B.; Kawanishi, Y.; Obata, T.; Tazuke, S. *J. Phys. Chem.* **1986**, *90*, 1488.
(8) Chang, Y. J.; Orman, L. K.; Anderson, D. R.; Yabe, T.; Hopkins, J. B. *J. Chem. Phys.* **1987**, *87*, 3249.
(9) Kober, E. M.; Sullivan, B. P.; Meyer, T. J. *J. Inorg. Chem.* **1984**, *23*, 2098.

0002-7863/90/1512-2612$02.50/0

studies, Raman spectra are interpreted in terms of complete localization, both above and below the glass transition temperature. While the evidence supporting the intrinsic localization model seems close to compelling, this question must be viewed as not fully resolved.

The question of the time scale on which exciton hopping occurs has also been discussed in the literature. Time-resolved and solvent-dependent[4,10,11] photoselection/emission polarization data have been interpreted in terms of nanosecond exciton hopping times. Later studies have shown, however, that this analysis is complicated by spin–lattice relaxation among the triplet sublevels of the emissive MLCT state.[12] Nanosecond transient Raman studies on mixed-ligand derivatives of $Ru^{II}(bpy)_3$ have shown that, in most cases, the optical electron is localized on the most easily reduced ligand.[14,15] This observation implies that exciton hopping takes place on the nanosecond or subnanosecond time scale. Consistent with this conclusion, Cooley et al. have reported picosecond emission kinetics for mixed-ligand derivatives of $Ru^{II}(bpy)_3$ in room-temperature acetonitrile, where one or more of the bipyridines is linked through a methylene chain to an electron acceptor. These results can be understood only if electron transfer occurs exclusively from the bipyridine nearest the electron acceptor, and if exciton hopping takes place in less than 100 ps.[16] In contrast, time-resolved Raman results have recently been reported on mixed ligand $Ru^{II}(bpy)_3$-type compounds which extend from the picosecond to the microsecond time scale.[17] No change in the Raman spectra are detected over this range, and it is concluded that exciton hopping takes place very slowly, longer than the microsecond time scale. Clearly, there is no consensus even on the order of magnitude of exciton hopping rates.

In this paper, we report excited-state polarized absorption kinetics of $Ru^{II}(bpy)_3$ in room-temperature water, methanol, and ethylene glycol solutions. The results show that the optical electron is intrinsically localized on a single ligand and provide a direct measure of the exciton hopping time. The basic idea of the experiment is as follows. Excitation to the MLCT state, with polarized picosecond light pulses, photoselects a specific Ru-bpy moiety of the $Ru^{II}(bpy)_3$ molecule. Following excitation, the polarization of the (photoselected) bipyridine radical anion π–π^* absorption is determined as a function of time. Unlike MLCT emission, this transition is always polarized along the long axis of the bipyridine radical anion, regardless of triplet sublevel populations. As a result, $bpy^{\bullet-}$ (π,π^*) absorption kinetics are independent of spin–lattice relaxation, which complicates the polarized emission kinetics. Two processes may depolarize the excited-state absorption: exciton hopping and rotational diffusion. In viscous solvents rotational diffusion is comparatively slow, and a fast decay, characteristic of the exciton hopping time, may be observed. Photoselection of a specific Ru-bpy moiety is only possible if the optical electron is intrinsically localized. If the optical electron is not intrinsically localized, then no fast component would be detected.

Experimental Section

The experimental apparatus used in this study is shown schematically in Figure 1. It is based upon an active/passive mode-locked Nd:YAG laser with a single pulse selector and amplifier system. Samples are excited with ~30 ps pulses of 460-nm light, generated by anti-Stokes Raman shifting the 532 nm second harmonic in a high-pressure methane cell. Typical excitation energies are 100 μJ/pulse, and the excitation beam is focussed to about a 1-mm spot size. This results in excitation of about 20–30% of the irradiated molecules. As such, saturation effects

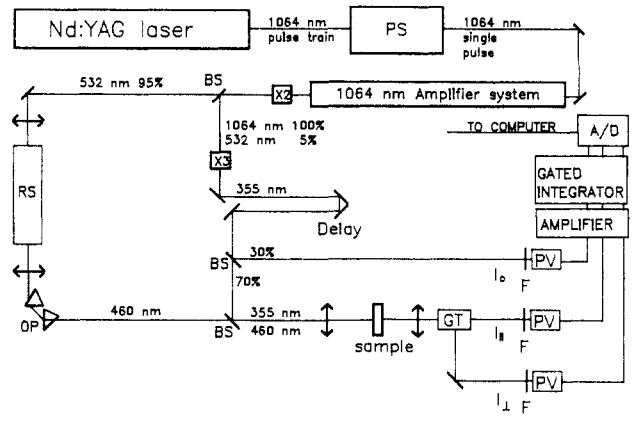

Figure 1. Experimental apparatus used to obtain the time-resolved polarization data. The following abbreviations are used: PS, pulse selector; BS, beam splitter; DP, dispersing prism; F, U360 filter; GT, Glan–Taylor polarizer; PV, photovoltaic; RS, high pressure methane Raman shifter. The double ended arrows indicate lenses.

are minimal. The excitation light is vertically polarized. Probe pulses (355 nm, 30 ps, ~10 μJ/pulse) are focussed to about 0.5 mm. A stepper motor driven variable delay controls the arrival time of the probe pulse. The arrival time of the probe pulse could be varied between −1 and 5 ns, relative to the arrival excitation pulse. The temporal instrument response function is determined by the convolution of the 30-ps excitation and probe pulses and is about 45 ps fwhm. The probe light is approximately randomly polarized at the sample, and the horizontal and vertical components are separated by a Glan–Taylor immediately thereafter. Reference, perpendicular, and parallel polarized beams are passed through diffusers prior to detection. Three EGG UV-100-BQ photovoltaics are used for detection. A U360 filter is placed before each detector, making the photovoltaics blind to scattered sample excitation and other sources of extraneous light. The output of each photovoltaic is amplified, integrated, and digitized on each laser shot. Digitized signals are stored in an IBM PC/AT computer, which also controls the firing of the laser and the movement of the delay stage. Typically, 20–50 laser shots are taken at each delay at a repetition rate of ~3 Hz.

$Ru(bpy)_3$ sample concentrations are typically 0.1–0.15 mM and are contained in 2-mm path length optical cells. $Ru(bpy)_3Cl_2$ was a gift from Professor C. M. Elliott and was prepared and purified by previously reported methods.[18] All solvents are reagent grade and used without further purification. All samples are degassed by several cycles of freeze–pump–thaw and sealed prior to use. The data reported here were obtained at room temperature.

Results and Discussion

A. Absorption Polarization Spectroscopy of $Ru^{II}(bpy)_3$*. The interpretation of time-resolved absorption polarization experiments depends crucially on the polarizations of the excited and detected transitions. Excitation (460 nm) directly populates the MLCT state. The excited state has a strong absorption band centered near 355 nm and is probed at that wavelength. The polarizations of these transitions are discussed below.

The lowest excited state of $Ru^{II}(bpy)_3$ is largely MLCT in nature[1] and is best described as $Ru^{III}(bpy)_2(bpy^{\bullet-})$. The polarization of this transition has been thoroughly studied by polarized emission experiments, and it was concluded that optical absorption leads to a state in which the transferred electron is intrinsically localized on a single ligand.[12] The initially populated state is a singlet which rapidly intersystem crosses to a triplet, without changing the ligand on which the optical electron is localized. The MLCT transition is polarized along the z-axis of the Ru–bpy, extending from the metal through the middle of the bipyridine ligand (see Figure 2A). Absorption of linearly polarized light selectively excites those Ru–bpy moieties whose z-axes are most closely aligned with the polarization (E field) vector of the light. It is important to note that since the MLCT state is intrinsically localized on the specific ligand, photoselection in the excitation process depends only on the orientation of individual Ru–bpy moieties (xyz coordinates).

(10) Carlin, C. M.; DeArmond, M. K. *J. Am. Chem. Soc.* **1985**, *107*, 53.
(11) Myrick, M. L.; Blakley, R. L.; DeArmond, M. K. *J. Am. Chem. Soc.* **1987**, *109*, 2841.
(12) Myrick, M. L.; Blakley, R. L.; DeArmond, M. K.; Arthur, M. L. *J. Am. Chem. Soc.* **1988**, *110*, 1325.
(13) Carrol, P. J.; Brus, L. E. *J. Am. Chem. Soc.* **1987**, *109*, 7613.
(14) McClanahan, S. F.; Dallinger, R. F.; Holler, F. J.; Kincaid, J. R. *J. Am. Chem. Soc.* **1985**, *107*, 4853.
(15) Mabrouk, P. A.; Wrighton, M. S. *Inorg. Chem.* **1986**, *25*, 526.
(16) Cooley, L. F.; Headford, C. E. L.; Elliott, C. M.; Kelley, D. F. *J. Am. Chem. Soc.* **1988**, *110*, 6673.
(17) Orman, L. K.; Change, Y. J.; Anderson, D. R.; Yabe, T.; Xu, X.; Yu, S.-C.; Hopkins, J. B. *J. Chem. Phys.* **1989**, *90*, 1469.
(18) Elliott, C. M.; Hershenhart, E. J. *J. Am. Chem. Soc.* **1982**, *104*, 7519.

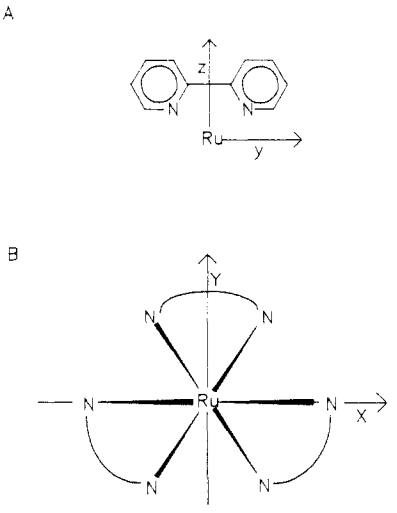

Figure 2. Coordinate axes used to describe (a) the Ru–bpy moiety and (b) the $Ru(bpy)_3$ molecule. This coordinate system is the same as that used in ref 12.

Due to mixing with higher electronically excited states, some relatively small component of the 460 nm absorption may not be z-axis polarized. While this relatively small component may be ignored in the qualitative interpretation of polarization data, quantitative interpretation requires that it be taken into account. The extent to which the 460-nm absorption is z-axis polarized can be estimated from emission polarization data on the analogous system, $Ru^{II}(bpy)(pyridine)_4$, where only a single electron-accepting ligand is present.

In general, the emission polarization is defined by

$$P = \frac{I_{\parallel} - I_{\perp}}{I_{\parallel} + I_{\perp}} \tag{1a}$$

where $I_{\parallel}$ and $I_{\perp}$ are the emission intensities polarized parallel and perpendicular, respectively, to the polarization of the incident light. The relative intensities of $I_{\parallel}$ and $I_{\perp}$ may be calculated if the relative orientation of the emission and absorption oscillators is known. Photoselection theory has been discussed in detail by Albrecht,[19] and the equations in ref 19 are used throughout this paper to calculate polarization values. If the oscillators are collinear, as would be expected for a system with only one low-lying MLCT transition such as $Ru^{II}(bpy)(pyridine)_4$, then a value of $P = 1/2$ is calculated. Myrick et al. have obtained an experimental value of ~ 0.4 for the emission polarization following 460-nm absorption.[12] Since this value is not very different from the predicted value of $1/2$, it indicates that most of the absorption is indeed polarized along the z axis. If the remainder of the absorption is assumed to be unpolarized, then from photoselection theory[19] we calculate that 77% of the absorption is z-axis polarized (see Appendix). We expect that about the same fraction (23%) of unpolarized 460-nm absorption will be present in $Ru^{II}(bpy)_3$.

Following MLCT excitation, one of the bipyridines has an electron in its π system and is essentially a bipyridine radical anion. As a result, $Ru^{II}(bpy)_3^*$ has a near ultraviolet absorption spectrum[20,21] which shows the same bands as the unbound bipyridine radical anion. This spectrum is also quite similar to that of the electrochemically reduced species[22] $Ru(bpy)_3^{1+}$, which ESR studies have shown to have an electron localized on a single ligand.[23] The bipyridine radical anion exhibits an intense ($\epsilon \simeq 2 \times 10^4$ cm^{-1} M^{-1}) absorption with a maximum at 380 nm. This absorption has been assigned to a $\sigma_6 \rightarrow \sigma_7$ (highest π to lowest π^*) transition.[24,25] Elementary group theoretical considerations show that this transition is polarized along the long axis of the bipyridine, i.e., the y axis in Figure 2A. The maximum absorbance in $Ru^{II}(bpy)_3^*$ is shifted about 20 nm to the blue of that in the free bipyridine radical anion, indicating the presence of a weaker, overlapping electronic transition.[20] As in the case of the MLCT absorption oscillator, this weak transition may be ignored in the qualitative, but not quantitative, interpretation of the polarization data. The presence of this transition in the excited-state spectrum, but not in the bipyridine radical anion or $Ru^{III}(bpy)_3$ spectra,[26] suggests that it may be assigned to a charge-transfer transition associated with the Ru^{III}-$bpy^{\bullet-}$ moiety and is therefore z-axis polarized. Thus, at 355 nm, $Ru^{II}(bpy)_3^*$ has two transitions, both of which are associated with a single bipyridine ligand: a strong one, which is y-axis polarized and a much weaker one which is probably z-axis polarized.

As stated above, excitation with linearly polarized 460 nm light largely photoselects those Ru–bpy moieties which are most closely aligned with the polarization vector of the light. Since the ground state of $Ru^{II}(bpy)_3$ has comparatively little absorbance at 355 nm, almost all of the absorption of this wavelength is associated with the nascent Ru^{III}-$bpy^{\bullet-}$ moiety. Immediately following MLCT excitation, most of 355 nm absorbance is polarized perpendicular to the polarization of the 460 nm light. Just as in the emission case, the absorption polarization is given by

$$P = \frac{A_{\parallel} - A_{\perp}}{A_{\parallel} + A_{\perp}} \tag{1b}$$

where $A_{\parallel}$ and $A_{\perp}$ are the transient absorptions which are polarized parallel and perpendicular, respectively, to the polarization of the excitation light. The polarization may be calculated for linearly polarized excitation light, assuming that neither exciton hopping nor rotational diffusion has occurred. From the Appendix, the value of P, prior to exciton hopping, is given by

$$P_{\text{prior}} = \frac{6\beta - 9\alpha\beta}{10 + 2\beta - 3\alpha\beta} \tag{2}$$

where α is the fraction of the 355-nm absorbance which is y-axis polarized, and the remaining $(1 - \alpha)$ absorbance is assumed to be z-axis polarized. Similarly, β is the fraction of the 460-nm ground-state absorbance polarized along the z-axis, and the remaining $(1 - \beta)$ absorbance is assumed to be unpolarized; for $Ru^{II}(bpy)_3$, β is taken to be 0.77. The polarization may also be calculated assuming that the exciton has been randomized among the bipyridine ligands, but no rotational diffusion has occurred. The polarization following excitation hopping (see Appendix) is given by

$$P_{\text{following}} = \frac{3\beta + 6\alpha\beta}{20 + \beta - 2\alpha\beta} \tag{3}$$

Immediately following excitation (prior to exciton hopping or rotational diffusion) a value of P given by eq 2 is expected. If exciton hopping is fast compared to rotational diffusion, then a value of P given by eq 3 is expected after exciton hopping has randomized the exciton among the ligands. Finally, on a longer time scale, the polarization will decay to zero as rotational diffusion proceeds.

The time dependence of the extent to which the absorption is polarized is most conveniently given in terms of the depolarization ratio

$$r = \frac{A_{\parallel} - A_{\perp}}{A_{\parallel} + 2A_{\perp}} = \frac{2P}{3 - P} \tag{4}$$

The time dependence of r is given by

$$r(t) = C_1 \exp(-(6D_s + 3k_h)t) + C_2 \exp(-6D_s t) \tag{5a}$$

(19) Albrecht, A. C. *M. Molec. Spec.* **1961**, *6*, 84.
(20) Creutz, C.; Chou, M.; Metzel, T. L.; Okumura, M.; Satin, N. *J. Am. Chem. Soc.* **1980**, *102*, 1309.
(21) Hauser, A.; Krausz, E. *Chem. Phys. Lett.* **1987**, *138*, 355.
(22) Heath, G. A.; Yellowlees, L. J. *J. Chem. Soc., Chem. Commun.* **1981**, 287. Coombe, V. T.; Heath, G. A.; MacKenzie, A. J.; Yellowlees, L. J. *Inorg. Chem.* **1984**, *23*, 3423.
(23) Motten, A. G.; Hanck, K.; DeArmond, M. K. *Chem. Phys. Lett.* **1981**, *79*, 541. Morris, D. E.; Hanck, K. W.; DeArmond, M. K. *J. Am. Chem. Soc.* **1983**, *105*, 3032.
(24) Konig, E.; Kemmer, S. *Chem. Phys. Lett.* **1970**, *5*, 87.
(25) Ohsawa, Y.; Whangbo, M.-H.; Hanck, K. W.; DeArmond, M. K. *Inorg. Chem.* **1984**, *23*, 3426.
(26) Paulson, S.; Elliott, C. M. Unpublished results.

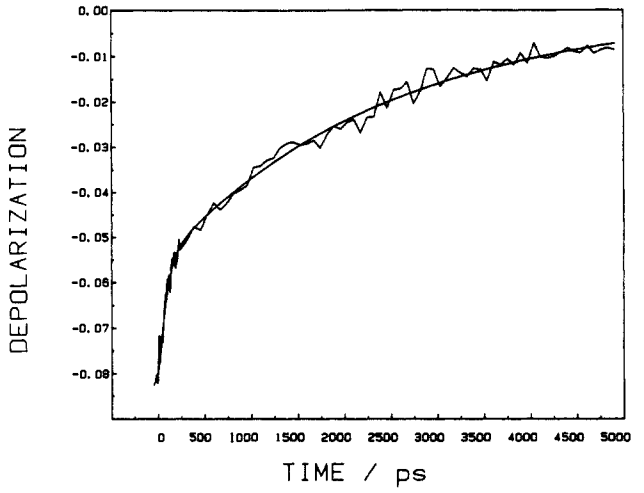

Figure 3. Experimental plot of the depolarization ratio obtained for $Ru^{II}(bpy)_3$ in room-temperature ethylene glycol. Also shown is a calculated curve corresponding to a biphasic (75 ps, 2.4 ns) depolarization decay. The amplitudes of the calculated fast and slow decay components are −0.03 and −0.056, respectively. The curve was calculated from the convolution of the absorbances with the known instrument temporal response function.

where D_s is the rotational diffusion constant and k_h is the bipyridine-to-bipyridine exciton hopping rate constant.[10,27] The factor of three differences between the ligand-to-ligand exciton hopping rate and the depolarization decay rate comes from the fact that hopping can occur to either of two other ligands and follows directly from the solution of the rate equations. D_s can be related to the molecular hydrodynamic radius and the solvent viscosity by eq 5b. This equation assumes that $Ru^{II}(bpy)_3^*$ is

$$D_s = \frac{kT}{8\pi\eta r^3} \tag{5b}$$

roughly spherical and may therefore be described by a single rotational diffusion constant, D_s, which is surely a good approximation. The values of C_1 and C_2 may be calculated from eq 2–4 once the value of α has been determined. Following exciton hopping, the first term in eq 5a can be ignored, and we get

$$C_2 = \frac{2P_{\text{following}}}{3 - P_{\text{following}}} \tag{6a}$$

At $t = 0$ (prior to exciton hopping) $r = C_1 + C_2$, and we get

$$C_1 = \frac{2P_{\text{prior}}}{3 - P_{\text{prior}}} - C_2 \tag{6b}$$

The values of α and β (= 0.77) and therefore C_1 and C_2 are determined by the electronic structure of $Ru^{II}(bpy)_3$ and are expected to be very close to the same in all solvents.

B. Time-Resolved Results in Ethylene Glycol. Figure 3 shows an experimental plot of $r(t)$ obtained in room-temperature ethylene glycol. Two components of the decay are clearly visible. Also shown is a calculated curve corresponding to biexponential decay with 75 ps and 2.4 ns components. This curve is obtained by convolving calculated parallel and perpendicular absorption curves with the known instrument response function and subsequently calculating the time dependent depolarization ratio. The long component is assigned to rotational diffusion. Given that ethylene glycol is relatively viscous (~18 cP at 22 °C), this time scale is consistent with the decay times observed in other molecules of comparable size.[27] Indeed, a 2.4 ns decay corresponds to a hydrodynamic radius of 5.2 Å, which is quite reasonable for $Ru^{II}(bpy)_3$. The 75-ps component is assigned to exciton hopping and corresponds to an exciton hopping rate of 230 ps^{-1} between any two bipyridine ligands (eq 5a).

The amplitudes of the fast and slow components (−0.03 and −0.056, respectively) of the calculated curve in Figure 3 are determined from eq 6, with α and β values of 0.87 and 0.77, respectively. It is important to note that β was determined from polarized emission studies and that a single value of α correctly gives the amplitudes of both the exciton hopping and rotational diffusion decay components. This quantitative agreement strongly supports the above assignments.

C. Solvent Relaxation and Exciton Hopping Rates. The 230 ps exciton hopping time obtained in ethylene glycol may be understood in terms of solvent relaxation dynamics. Recently, many theoretical studies have investigated the role of solvent dynamics in electron-transfer reactions.[28] Several general conclusions about when solvent dynamics will control the reaction rate have been reached and are briefly discussed here. In the absence of an energetic barrier, the electron-transfer time will be on the order of the solvent longitudinal relaxation time, τ_L. While in some cases this correspondence is quite close, in others it is only within an order of magnitude.[29] In solvents with more than one τ_L, electron transfer will largely be controlled by the fast relaxation dynamics.[30,31] In such cases, solvent dynamics are often characterized by an "effective" longitudinal relaxation time,[30] $\tau_{L,\text{eff}}$. Alternatively, in cases where there is a significant energetic barrier, the reaction will be slower and may or may not be controlled by solvent relaxation dynamics. In fact, when the barrier is sufficiently high and solvent relaxation is sufficiently fast, the rate is given by simple transition-state theory. An expression for the intermediate case, with weakly adiabatic coupling between the initial and final states, has been derived by Hynes[30]

$$k_h = \left[1 + \frac{2k^{TST}}{k_d}\right]^{-1} k^{TST} \tag{7}$$

where k^{TST} is the transition-state theory (TST) rate, and k_d is the rate of solvent relaxation. If there is no solvent-induced barrier to reaction, then k_d will be on the order of $1/\tau_L$. k^{TST} may be given by the usual expression: $k^{TST} = (kT/h)\exp(-\Delta G^*/RT)$. In eq 7, the electron-transfer reaction is considered to be a two-step process: first, reorganization of the solvent to a configuration where electron transfer can take place and, second, surmounting the energetic barrier. Either of these processes may be rate-limiting.

The relaxation dynamics of ethylene glycol have been studied, using time and wavelength resolved emission of 4,4′-(dimethylamino)phenylsulfone as a probe. In these studies, the emission spectral shift correlation function was fit to a 100-ps decay, in agreement with the 86-ps value of τ_L determined from dielectric measurements.[28a] The correlation function, however, shows both longer and shorter decay components. The reported 100 ps value corresponds to an effective decay time[32] and provides a reasonable approximation to the value of $\tau_{L,\text{eff}}$. Since this value is on the order of the observed 230 ps exciton hopping time, we conclude that the reaction is largely controlled by solvent dynamics, i.e., solvent relaxation is the rate-limiting process. This also suggests that the reaction has little solvent-induced barrier (less than a few kT). However, the reaction may be controlled by the fast components of the ethylene glycol relaxation dynamics. If this is the case, then the presence of a significant solvent-induced barrier (several kT) is indicated by the observed 230 ps exciton hopping time. In the absence of detailed dynamical data (i.e., spectral shift correlation functions which resolve the magnitude and decay rates of the fast components) on ethylene glycol, the role of the fast

(27) Fleming, G. *Chemical Applications of Ultrafast Spectroscopy*; Oxford, 1986; Chapter 6.

(28) For recent reviews see: (a) Simon, J. D. *Acc. Chem. Res.* **1988**, *21*, 128. (b) Barbara, P. F.; Jarzeba, W. *Acc. Chem. Res.* **1988**, *21*, 195. (c) Barbara, P. F.; Kang, T. J.; Jarzeba, W.; Fonseca, T. In *Perspectives in Photosynthesis*; Reidel: D. Dordrecht, Holland, 1990.

(29) Kahlow, M. A.; Kang, T. J.; Barbara, P. F. *J. Phys. Chem.* **1987**, *91*, 6452.

(30) Hynes, J. T. *J. Phys. Chem.* **1986**, *90*, 3701.

(31) Calef, D. F.; Wolynes, P. G. *J. Phys. Chem.* **1983**, *87*, 3387. *J. Chem. Phys.* **1983**, *78*, 470.

(32) Simon, J. D. Private communication, unpublished results.

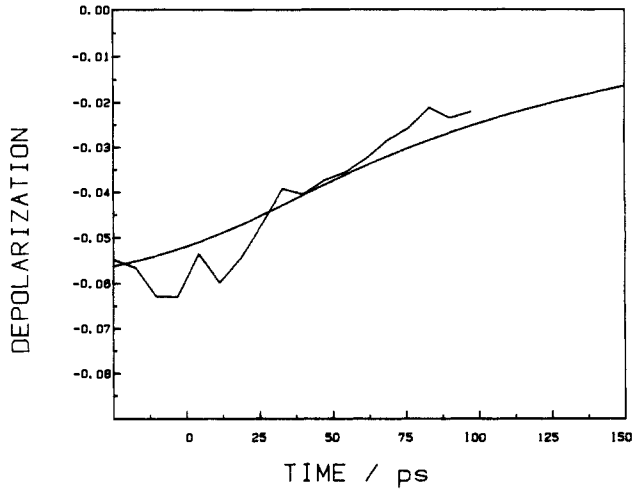

Figure 4. Experimental plot of the depolarization ratio obtained in room-temperature water. Also shown is a calculated curve corresponding to the convolution of the known instrument response with a biphasic (5 and 125 ps) depolarization decay. The amplitudes and decay times are determined in eq 5–7 in the text, with no adjustable parameters.

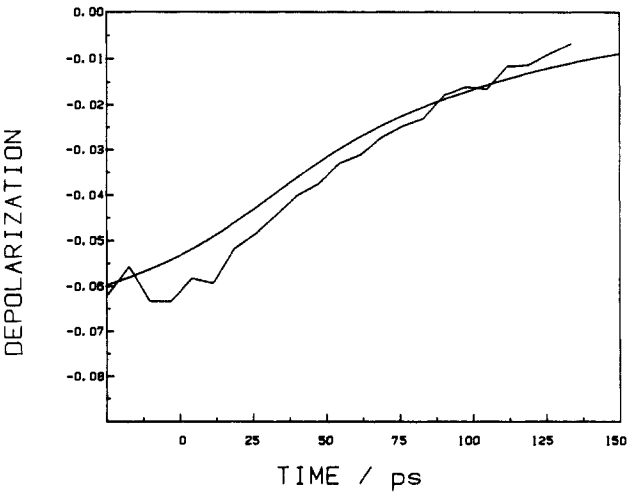

Figure 5. Experimental plot of the depolarization ratio obtained in room-temperature methanol. Also shown is a calculated curve corresponding to the convolution of the known instrument response with a biphasic (9 and 75 ps) depolarization decay. The amplitudes and decay times are determined in eq 5–7 in the text, with no adjustable parameters.

relaxation components on the electron-transfer rate cannot be determined.[33]

The above analysis does not preclude the existence of a significant internal (vibrational) barrier to exciton hopping, which corresponds to the amount of vibrational excitation needed to facilitate the reaction. The magnitude of the total (internal plus solvent induced) barrier can be estimated from data obtained for the electrochemically reduced species, $Ru(bpy)_3^{1+}$. This species is quite similar to $Ru^{II}(bpy)_3^*$ in that both have an electron which is localized and can hop from one ligand to another. Temperature-dependent ESR line width studies[23] indicate that the electron hopping activation energy is about 960 cm^{-1}, and a similar value would be expected for $Ru^{II}(bpy)_3^*$. From this value, a TST rate of $(15\ ps)^{-1}$ is calculated, which is considerably faster than the solvent relaxation rate. With this TST rate and a value of $k_d = 1/\tau_L = (100\ ps)^{-1}$, eq 7 yields an electron-transfer time of 215 ps, which closely matches the observed 230 ps exciton hopping time.

Depolarization ratio decays may be calculated for $Ru^{II}(bpy)_3^*$ in other solvents with eq 5–7. If the same value of ΔG^* (= 960 cm^{-1}) is used to obtain a TST theory rate, then this calculation involves no adjustable parameters; everything is determined. Values of C_1 and C_2 are determined from the solvent-independent values of α and β ($\alpha = 0.87$, $\beta = 0.77$) and are −0.03 and −0.056, respectively, just as in ethylene glycol. Values of D_s in water and methanol are calculated from the known (5.2 Å) hydrodynamic radius and the respective solvent viscosities. Equation 7 may then be evaluated if k_d^{-1} is taken to be the effective longitudinal relaxation time, and k^{TST} is again taken to be $(15\ ps)^{-1}$. Taking k^{TST}, and therefore ΔG^*, to be solvent independent is consistent with the idea that the barrier is largely due to internal motions.

Water has an effective longitudinal relaxation time of <1 ps, and k_D is estimated to be $>10^{12}\ s^{-1}$. Since this is much greater than the TST rate of $(15\ ps)^{-1}$, the rate of exciton hopping in water should be given by TST: $k_h = k^{TST} = (15\ ps)^{-1}$. Figure 4 shows the experimental data obtained in room-temperature water and a curve calculated from the above model with no adjustable parameters. Water has a much lower viscosity than ethylene glycol (0.9 compared to 18 cP), and rotational diffusion proceeds much faster. As a result of this and the finite temporal response of the laser system, some, but not all, of the ability to resolve the depolarization due to exciton hopping is lost. Despite this caveat, reasonable agreement between the experimental and calculated results is obtained.

Methanol has an effective longitudinal relaxation time of about 6 ps, which is comparable to the TST reaction time.[28c] Exciton hopping is thus neither given by TST nor is entirely controlled by solvent dynamics. Equation 7 gives and exciton hopping time of 27 ps. Figure 5 shows the experimental results and a curve calculated from the above model.

While reasonable agreement between the calculated and experimental results is obtained in Figures 4 and 5, in both cases the calculations predict a somewhat smaller initial depolarization ratio than is actually observed. However, if a slightly lower value of k^{TST} is assumed, then, due to the convolution with the instrument temporal response, a larger amplitude is calculated. A value of $k^{TST} = (45\ ps)^{-1}$, corresponding to a ΔG^* value of 1185 cm^{-1}, is needed to correctly fit the amplitude of the experimental curve. This is still quite close to the 960 cm^{-1} value obtained for $Ru(bpy)_3^{1+}$.

Conclusions

Several important conclusions may be drawn from these studies: (1) Time-resolved absorption polarization techniques may be used to determine exciton hopping rates in metal $(diimine)_3$-type complexes. (2) The depolarization ratio observed for $Ru^{II}(bpy)_3^*$ dissolved in ethylene glycol exhibits a biphasic decay, with 75 ps and 2.4 ns components. The slow component is assigned to rotational diffusion. The fast component is assigned to exciton hopping, and its presence indicates that the optical electron is intrinsically localized on a single ligand. The 75-ps decay corresponds to a bipyridine-to-bipyridine exciton hopping rate of $(230\ ps)^{-1}$. Exciton hopping in water and methanol solutions occurs much faster (tens of picoseconds) but is still resolvable with the current laser system. (3) Exciton hopping rates in ethylene glycol, water, and methanol may be interpreted in terms of solvent-mediated electron-transfer theory. Due to slow solvent dynamics, exciton hopping in ethylene glycol is controlled by the rate of solvent relaxation. Theory predicts that the rate of exciton hopping in water should be given by transition-state theory, since in this case solvent dynamics are relatively fast. Exciton hopping in methanol is predicted to be an intermediate case. The experimental results obtained in this work are consistent with these predictions.

Clearly, better data in the more rapidly relaxing solvents is needed to develop a complete theoretical picture of the exciton hopping process. Slowing the rate of rotational diffusion would facilitate obtaining these data. This may be accomplished synthetically by attaching bulky groups to the bipyridines, thereby increasing the hydrodynamic radius. These studies as well as studies on mixed-ligand compounds are currently in progress and will be reported in later papers.

Acknowledgment. This work was supported by the National Science Foundation. We thank Professor C. M. Elliot for the gift

(33) Fonseca, T. *J. Chem. Phys.* **1989**, *91*, 2869.

of $Ru(bpy)_3Cl_2$ and for helpful discussions.

Appendix

In general, the absorption polarization is given as

$$P = \frac{A_\parallel - A_\perp}{A_\parallel + A_\perp} \tag{A1}$$

For linearly polarized excitation light, $A_\parallel$ and $A_\perp$ can be given in terms of the projections of the excitation and probe oscillators on the molecular axes. Specifically[19]

$$A_\parallel = 3(r_xq_x + r_yq_y + r_zq_z) + q_x(r_y + r_z) + q_y(r_x + r_z) + q_z(r_x + r_y)$$

$$A_\perp = r_xq_x + r_yq_y + r_zq_z + 2[q_x(r_y + r_z) + q_y(r_x + r_z) + q_z(r_x + r_y)] \tag{A2}$$

where r and q values are the respective absorption and probe relative oscillator strengths along the molecular axes. We have that $r_x + r_y + r_z = q_x + q_y + q_z = 1$. These equations allow us to evaluate the fraction of the 460-nm absorbance which is z-axis polarized, β, in $Ru^{II}(bpy)(pyridine)_4$. In this case, using the coordinate system in Figure 2A, we get $r_z = \beta + (1 - \beta)/3$, $r_x = r_y = (1 - \beta)/3$. We will assume that all the emission oscillator is z-axis polarized: $q_z = 1$, $q_x = q_y = 0$. This assumption is consistent with the observation that the polarization is independent of wavelength.[12] Taking P to be the experimentally observed emission polarization with 460-nm excitation ($P = 0.4$), from eq A1 and A2, we get

$$P = 0.4 = 3\beta/(5 + \beta) \quad \text{or} \quad \beta = 0.77$$

The same fraction is assumed to be z-axis polarized in each Ru–bpy moiety of $Ru^{II}(bpy)_3$.

To calculate the absorption polarization in $Ru^{II}(bpy)_3$ prior to exciton hopping, the "molecule" is taken to be a specific Ru–bpy moiety, and, as shown in the $Ru^{II}(bpy)(pyridine)_4$ case, the coordinate system is shown in Figure 2A. Again, we have $r_x = r_y = (1 - \beta)/3$ and $r_z = \beta + (1 - \beta)/3$. Similarly, for the probe absorbance $q_y = \alpha$, $q_z = 1 - \alpha$, $q_x = 0$, i.e., the fractions α and $1 - \alpha$ are polarized along with the y- and z-axes, respectively. The use of these values in eq A1 and A2 gives eq 2 in the text:

$$P_{\text{prior}} = \frac{6\beta - 9\alpha\beta}{10 + 2\beta - 3\alpha\beta}$$

Following exciton hopping all three z-axes are equivalent, and the coordinate systems of the entire $Ru^{II}(bpy)_3$ molecule must be used. Because all three z-axes lie in the XY plane, this situation is equivalent to stating that excitation is largely in the XY plane (see Figure 2B). As before, the major (α) and the minor ($1 - \alpha$) components of the 355-nm absorption are taken along the y- and z-axes, respectively. The rotationally averaged projections of the Ru–bpy moiety (x,y,z) axes on the $Ru^{II}(bpy)_3$ (X,Y,Z) coordinate system have been calculated[12] and are as follows: $|x\cdot X|^2_{av} = |x\cdot Y|^2_{av} = |x\cdot Z|^2_{av} = 1/3$, $|y\cdot X|^2_{av} = |y\cdot Y|^2_{av} = 1/6$, $|y\cdot Z|^2_{av} = 2/3$ $|z\cdot Y|^2_{av} = |z\cdot X|^2_{av} = 1/2$, $|z\cdot Z|^2_{av} = 0$. By using these projections we can calculate r and q values which correspond to molecule following exciton hopping. For example,

$$r_X(\text{following}) = |x\cdot X|^2_{av}r_x + |y\cdot X|^2_{av}r_y + |z\cdot X|^2_{av}r_z$$

$$= (1/3)(1 - \beta)/3 + (1/6)(1 - \beta)/3 + (1/2)(\beta + (1 - \beta))/3$$

$$= 1/3 + \beta/6$$

Similarly,

$$r_y(\text{following}) = 1/3 + \beta/6$$

$$r_z(\text{following}) = (1 - \beta)/3$$

$$q_x(\text{following}) = q_y(\text{following}) = 1/2 - \alpha/3$$

$$q_z(\text{following}) = 2\alpha/3$$

By using these values in eq A2, we get eq 3 in the text

$$P_{\text{following}} = \frac{3\beta - 6\alpha\beta}{20 + \beta - 2\alpha\beta}$$

This equation may also be obtained by considering the projections of the (xyz) axes of the other (not photoselected) bipyridines on the photoselected bipyridine (xyz) coordinate system.